3. ATMOSPHERIC ABSORPTION

At frequencies above 2 GHz attenuation of radio waves due to absorption or scattering by constituents of the atmosphere, and by particles in the atmosphere, may seriously affect microwave relay links, communication via satellites, and radio and radar astronomy. At frequencies below 1 GHz the total radio wave absorption by oxygen and water vapor for propagation paths of 1000 kilometers or less will not exceed 2 decibels. Absorption by rainfall begins to be barely noticeable at frequencies from 2 to 3 GHz, but may be quite appreciable at higher frequencies.

For frequencies up to 100 GHz, and for both optical and transhorizon paths, this section provides estimates of the long-term median attenuation A_a of radio waves by oxygen and water vapor, the attenuation A_r due to rainfall, and the order of magnitude of absorption by clouds of a given water content. The estimates are based on work reported by Artman and Gordon [1954], Bean and Abbott [1957], Bussey [1950], Crawford and Hogg [1956], Gunn and East [1954], Hathaway and Evans [1959], Hogg and Mumford [1960], Hogg and Semplak [1961], Lane and Saxton [1952], Laws and Parsons [1943], Perlat and Voge [1953], Straiton and Tolbert [1960], Tolbert and Straiton [1957], and Van Vleck [1947a, b; 1951].

3.1 Absorption by Water Vapor and Oxygen

Water vapor absorption has a resonant peak at a frequency of 22.23 GHz, and oxygen absorption peaks at a number of frequencies from 53 to 66 GHz and at 120 GHz. Figure 3.1, derived from a critical appraisal of the above references, shows the differential absorption γ_{oo} and γ_{wo} in decibels per kilometer for both oxygen and water vapor, as determined for standard conditions of temperature and pressure and for a surface value of absolute humidity equal to 10 grams per cubic meter. These values are consistent with those prepared for the Xth Plenary Assembly of the CCIR by U.S. Study Group IV [1963d] except that the water vapor density is there taken to be 7.5 g/m^3. For the range of absolute humidity likely to occur in the atmosphere, the water vapor absorption in db/km is approximately proportional to the water vapor density.

The total atmospheric absorption A_a decibels for a path of length r_o kilometers is commonly expressed in one of two ways, either as the integral of the differential absorption $\gamma(r)$ dr:

$$A_a = \int_0^{r_o} \gamma(r)\, dr \quad \text{db} \tag{3.1}$$

or in terms of an absorption coefficient $\Gamma(r)$ expressed in reciprocal kilometers:

$$A_a = -10 \log \exp\left[-\int_0^{r_o} \Gamma(r)\, dr\right] = 4.343 \int_0^{r_o} \Gamma(r)\, dr \quad \text{db}. \tag{3.2}$$

The argument of the logarithm in (3.2) is the amount of radiowave energy that is not absorbed in traversing the path.

The total gaseous absorption A_a over a line-of-sight path of length r_o kilometers is

$$A_a = \int_0^{r_o} dr\,[\gamma_o(h) + \gamma_w(h)] \quad \text{db} \tag{3.3}$$

where h is the height above sea level at a distance r from the lower terminal, measured along a ray path between terminals. For radar returns, the total absorption is $2A_a$ db.

Considering oxygen absorption and water vapor absorption separately, (3.3) may be written

$$A_a = \gamma_{oo} r_{eo} + \gamma_{wo} r_{ew} \quad \text{db} \tag{3.4}$$

where r_{eo} and r_{ew} are effective distances obtained by integrating γ_o/γ_{oo} and γ_w/γ_{wo} over the ray path.

The effective distances r_{eo} and r_{ew} are plotted versus r_o and frequency for elevation angles θ_o = 0, 0.01, 0.02, 0.05, 0.1, 0.2, 0.5, 1, and $\pi/2$ radians in figures 3.2-3.4. Figure 3.5 shows the relationship between r_o and the sea level arc distance, d, for these values of θ_o.

A_a may be estimated from figures I.21 to I.26 of annex I, where attenuation relative to free space, A, is plotted versus f, θ_o, and r_o, ignoring effects of diffraction by terrain.

For nonoptical paths, the ray from each antenna to its horizon makes an angle θ_{ot} or θ_{or} with the horizontal at the horizon, as illustrated in figure 6.1 of section 6. The horizon rays intersect at distances d_1 and d_2 from the transmitting and receiving terminals. The total absorption A_a is the sum of values A_{at} and A_{ar}

$$A_a = A_{at} + A_{ar} \tag{3.5}$$

where $$A_{at} \equiv A_a(f, \theta_{ot}, d_1), \quad A_{ar} \equiv A_a(f, \theta_{or}, d_2).$$

For propagation over a smooth earth, $\theta_{ot} = \theta_{or} = 0$, and $A_a \cong 2A_a(f, 0, d/2)$. For trans-horizon paths and the frequency range 0.1 - 10 GHz, figure 3.6 shows A_a plotted versus distance over a smooth earth between 10 meter antenna heights.

3.2 Sky-Noise Temperature

The nonionized atmosphere is a source of radio noise, with the same properties as a reradiator that it has as an absorber. The effective sky-noise temperature T_s may be determined by integrating the gas temperature T multiplied by the differential fraction of reradiated power that is not absorbed in passing through the atmosphere to the antenna:

$$T_s(°K) = \int_0^\infty T(r)\Gamma(r) \exp\left[-\int_0^r \Gamma(r')\, dr'\right] dr \qquad (3.6)$$

where the absorption coefficient $\Gamma(r)$ in reciprocal kilometers is defined by (3.2). For instance, assuming

$$T(r) = (288 - 6.5h)\,°K \quad \text{for} \quad h \leq 12 \text{ km},$$

and

$$T(r) = 210°K \qquad \text{for} \quad h \geq 12 \text{ km},$$

figure 3.7 shows the sky-noise temperature due to oxygen and water vapor for various angles of elevation and for frequencies between 0.1 and 100 GHz.

In estimating antenna temperatures, the antenna pattern and radiation from the earth's surface must also be considered.

3.3 Attenuation by Rain

The attenuation of radio waves by suspended water droplets and rain often exceeds the combined oxygen and water vapor absorption. Water droplets in fog or rain will scatter radio waves in all directions whether the drops are small compared to the wavelength or comparable to the wavelength. In the latter case, raindrops trap and absorb some of the radio wave energy; accordingly, rain attenuation is much more serious at millimeter wavelengths than at centimeter wavelengths.

In practice it has been convenient to express rain attenuation as a function of the precipitation rate R_r which depends on both the liquid water content and the fall velocity of the drops, the latter in turn depending on the size of the drops. There is little evidence that rain with a known rate of fall has a unique drop-size distribution, and the problem of estimating the attenuation of radio waves by the various forms of precipitation is quite difficult.

Total absorption A_r due to rainfall over a path of length r_o can be estimated by integrating the differential rain absorption $\gamma_r(r)\,dr$ along the direct path between two intervisible antennas, or along horizon rays in the case of transhorizon propagation:

$$A_r = \int_0^{r_o} \gamma_r(r)\,dr \text{ decibels.} \tag{3.7}$$

Fitting an arbitrary mathematical function empirically to theoretical results given by Hathaway and Evans [1959] and Ryde and Ryde [1945], the rate of absorption by rain γ_r may be expressed in terms of the rainfall rate R_r in millimeters per hour as

$$\gamma_r = K R_r^{\alpha} \quad \text{db/km} \tag{3.8}$$

for frequencies above 2 GHz. The functions $K(f_G)$ and $\alpha(f_G)$ are plotted in figures 3.8 and 3.9, where f_G is the radio frequency in GHz,

$$K = [\,3(f_G - 2)^2 - 2(f_G - 2)\,] \times 10^{-4} \tag{3.9a}$$

$$\alpha = [\,1.14 - 0.07(f_G - 2)^{\frac{1}{3}}\,]\,[\,1 + 0.085(f_G - 3.5)\exp(-0.006\, f_G^2)\,]. \tag{3.9b}$$

An examination of the variation of rainfall rate with height suggests a relation of the form

$$R_r/R_{rs} = \exp(-0.2\,h^2) \tag{3.10}$$

where R_{rs} is the surface rainfall rate. Then

$$A_r = \gamma_{rs} r_{er} \text{ db}, \tag{3.11}$$

$$\gamma_{rs} = KR_{rs}^{\alpha} \text{ db/km}, \qquad r_{er} = \int_0^{r_o} dr \exp(-0.2\,\alpha h^2) \text{ km} \tag{3.12}$$

where γ_{rs} is the surface value of the rate of absorption by rain, and r_{er} is an "effective rainbearing distance". Figures 3.10 -3.13 show r_{er} versus r_o for several values of θ_o and α. The curves shown were computed using (3.12).

A "standard" long-term cumulative distribution of rain absorption is estimated, using some statistics from Ohio analyzed by Bussey [1950], who relates the cumulative distribution of instantaneous path average rainfall rates for 25, 50, and 100-kilometer paths, respectively, with the cumulative distributions for a single rain gauge of half-hour, one-hour, and two-hour mean rainfall rates, recorded for a year. The total annual rainfall in Ohio is about 110 centimeters.

Rainfall statistics vary considerably from region to region, sometimes from year to year, and often with the direction of a path (with or across prevailing winds). For instance, in North America, east-west systems seem particularly vulnerable, as they lie along the path of frequent heavy showers.

For very long paths, the cumulative distribution of instantaneous path average rainfall rates, $\overline{R}_r$, depends on how R_r varies with elevation above the surface and upon the correlation of rainfall with distance along the path. Figure 3.14 provides estimates of the instantaneous path average rainfall rate $\overline{R}_r$ exceeded for 0.01, 0.1, 1, and 5 per cent of the year as a function of r_{er} and normalized to a total annual rainfall of 100 cm. To obtain A_r from (3.11), replace R_{rs} in (3.12) with $\overline{R}_r$ from figure 3.14, multiplied by the ratio of the total annual rainfall and 100 cm. These estimates are an extrapolation of the results given by Bussey [1950] and are intended to allow for the average variation of R_r with height, as given by (3.10) and allowed for in the definition of r_{er}, and for the correlation of surface rainfall rate R_{rs} with distance along the surface, as analyzed by Bussey.

3.4 Attenuation in Clouds

Cloud droplets are regarded here as those water or ice particles having radii smaller than 100 microns or 0.01 cm. Although a rigorous approach to the problem of attenuation by clouds must consider drop-size distribution, it is more practical to speak of the water content of clouds rather than the drop-size distribution. Reliable measurements of both parameters are scarce, but it is possible to make reasonable estimates of the water content, M, of a cloud from a knowledge of the vertical extent of the cloud and the gradients of pressure, temperature, and mixing ratio, which is the ratio of the mass of water vapor to the mass of dry air in which it is mixed. The absorption within a cloud can be written as

$$A_c = K_1 M \text{ db} \tag{3.13}$$

where A_c is the total absorption attenuation within the cloud, K_1 is an attenuation coefficient, values for which are given in table 3.1, and M is the liquid water content of the cloud, measured in grams per cubic meter. The amount of precipitable water, M, in a given pressure layer can be obtained by evaluating the average mixing ratio in the layer, multiplying by the pressure difference, and dividing by the gravity. Using this method of obtaining M and the values of K_1 from table 3.1, it is possible to get a fairly reliable estimate of the absorption of radio energy by a cloud.

Several important facts are demonstrated by table 3.1. The increase in attenuation with increasing frequency is clearly shown. The values change by about an order of magnitude from 10 to 30 GHz. Cloud attenuation can be safely neglected below 6 GHz. The data presented here also show that attenuation increases with decreasing temperature. These relations are a reflection of the dependence of the refractive index on both wavelength and temperature. The different dielectric properties of water and ice are illustrated by the difference in attenuation. Ice clouds give attenuations about two orders of magnitude smaller than water clouds of the same water content.

TABLE 3.1

One-Way Attenuation Coefficient, K_1, in db/km/gm/m^3

Temperature (°C)		Frequency, GHz, 33	24	17	9.4
Water Cloud	20	0.647	0.311	0.128	0.0483
	10	0.681	0.406	0.179	0.0630
	0	0.99	0.532	0.267	0.0858
	-8	1.25	0.684	0.34 (extrapolated)	0.112 (extrapolated)
Ice Cloud	0	8.74×10^{-3}	6.35×10^{-3}	4.36×10^{-3}	2.46×10^{-3}
	-10	2.93×10^{-3}	2.11×10^{-3}	1.46×10^{-3}	8.19×10^{-4}
	-20	2.0×10^{-3}	1.45×10^{-3}	1.0×10^{-3}	5.63×10^{-4}

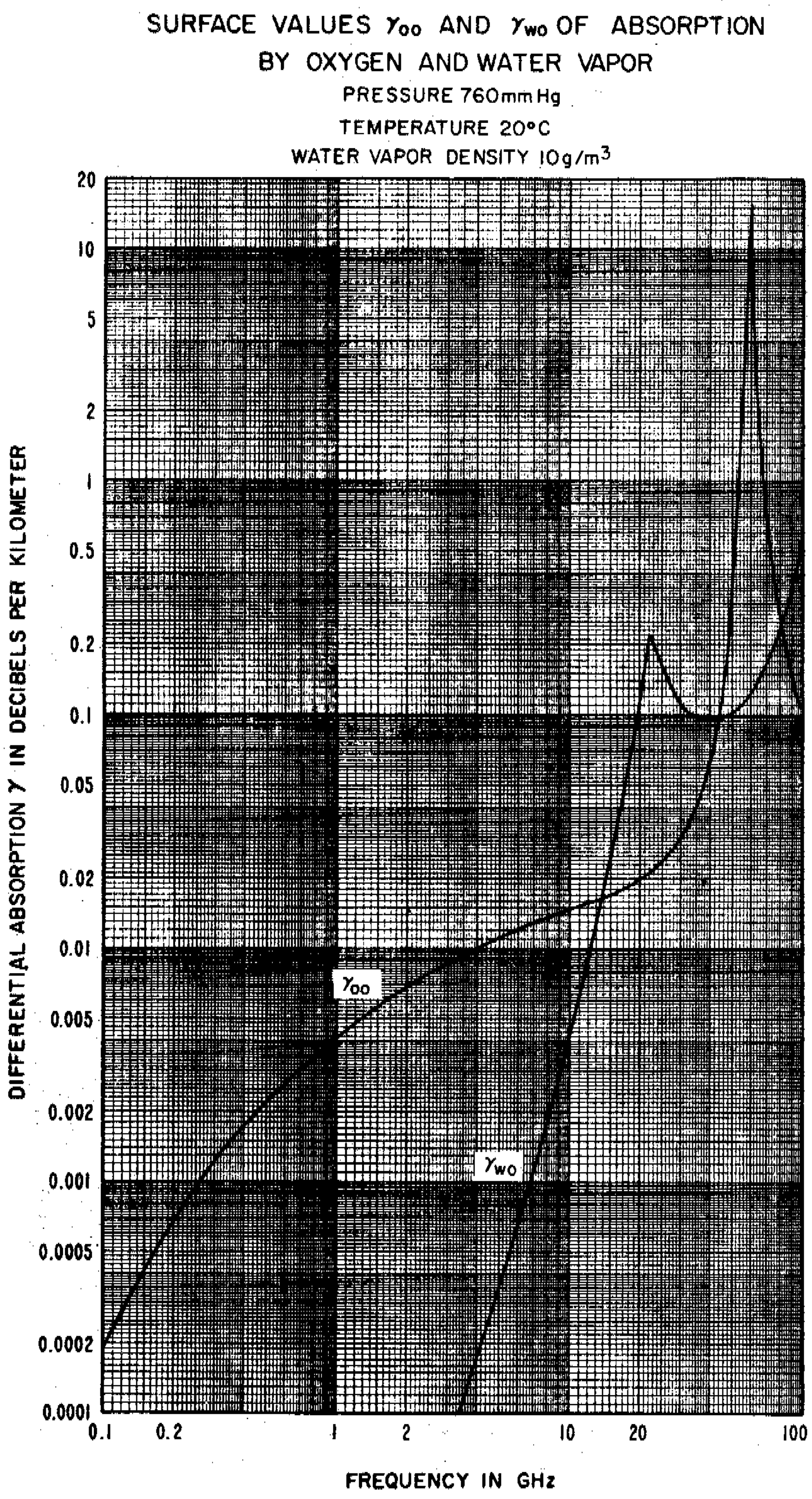
SURFACE VALUES γ_{oo} AND γ_{wo} OF ABSORPTION
BY OXYGEN AND WATER VAPOR
PRESSURE 760mm Hg
TEMPERATURE 20°C
WATER VAPOR DENSITY 10g/m³
DIFFERENTIAL ABSORPTION γ IN DECIBELS PER KILOMETER
20
10
5
2
1
0.5
0.2
0.1
0.05
0.02
0.01
0.005
0.002
0.001
0.0005
0.0002
0.0001
γ_{oo}
γ_{wo}
0.1
0.2
1
2
10
20
100
FREQUENCY IN GHz

Figure 3.1

EFFECTIVE DISTANCES r_{eo} AND r_{ew} FOR ABSORPTION BY OXYGEN AND WATER VAPOR

$\theta_0 = 0,\ 0.01,\ 0.02$

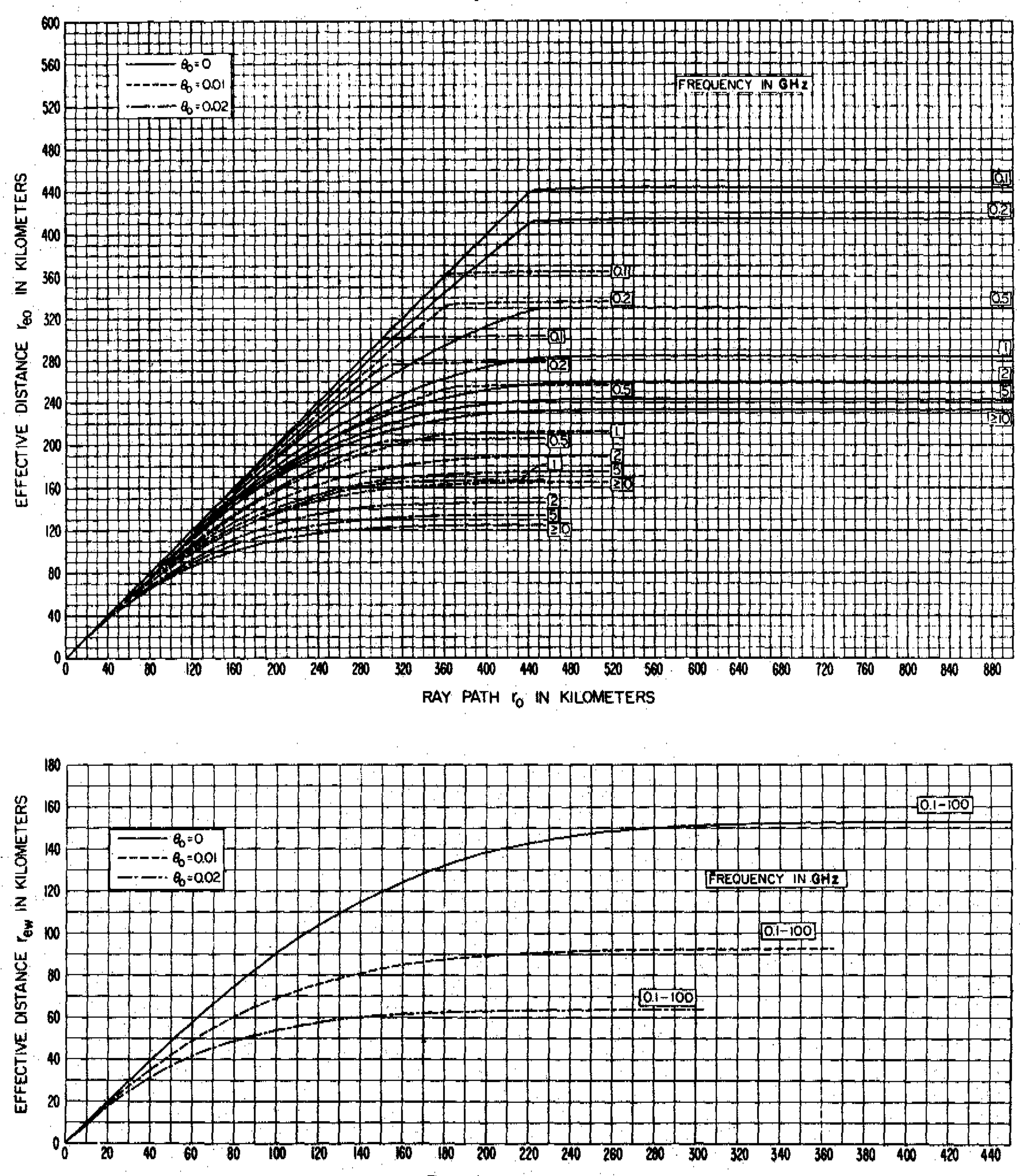

Figure 3.2

EFFECTIVE DISTANCES r_{eo} AND r_{ew} FOR ABSORPTION BY OXYGEN AND WATER VAPOR
θ_o = 0.05, 0.1, 0.2

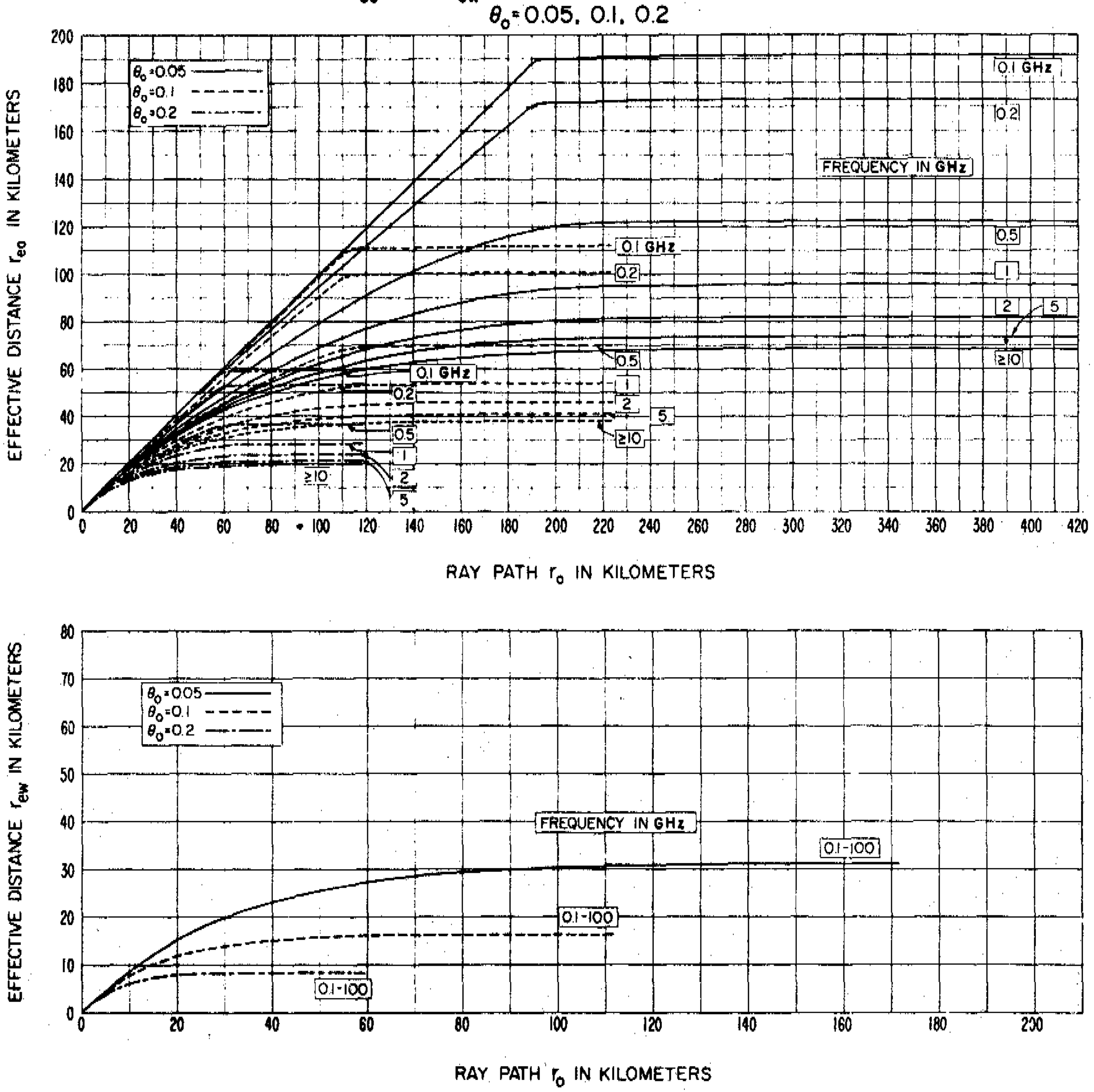

Figure 3.3

EFFECTIVE DISTANCES r_{eo} AND r_{ew} FOR ABSORPTION BY OXYGEN AND WATER VAPOR

$\theta_0 = 0.5, 1, \pi/2$

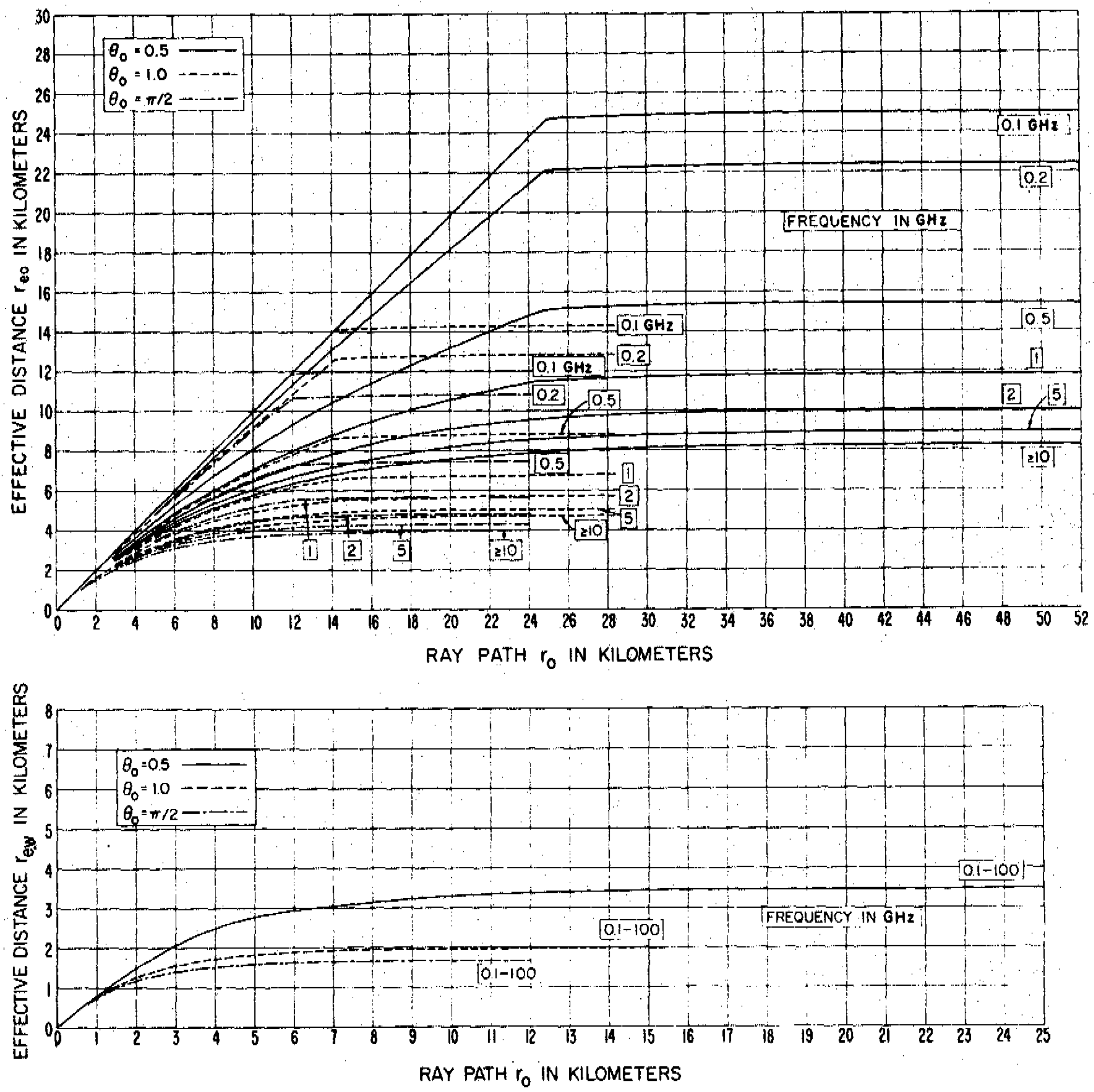

Figure 3.4

RAY PATH LENGTH, r_o, VERSUS SEA LEVEL ARC DISTANCE, d
θ_o = 0, 0.03, 0.1, 0.3, 0.5, 1

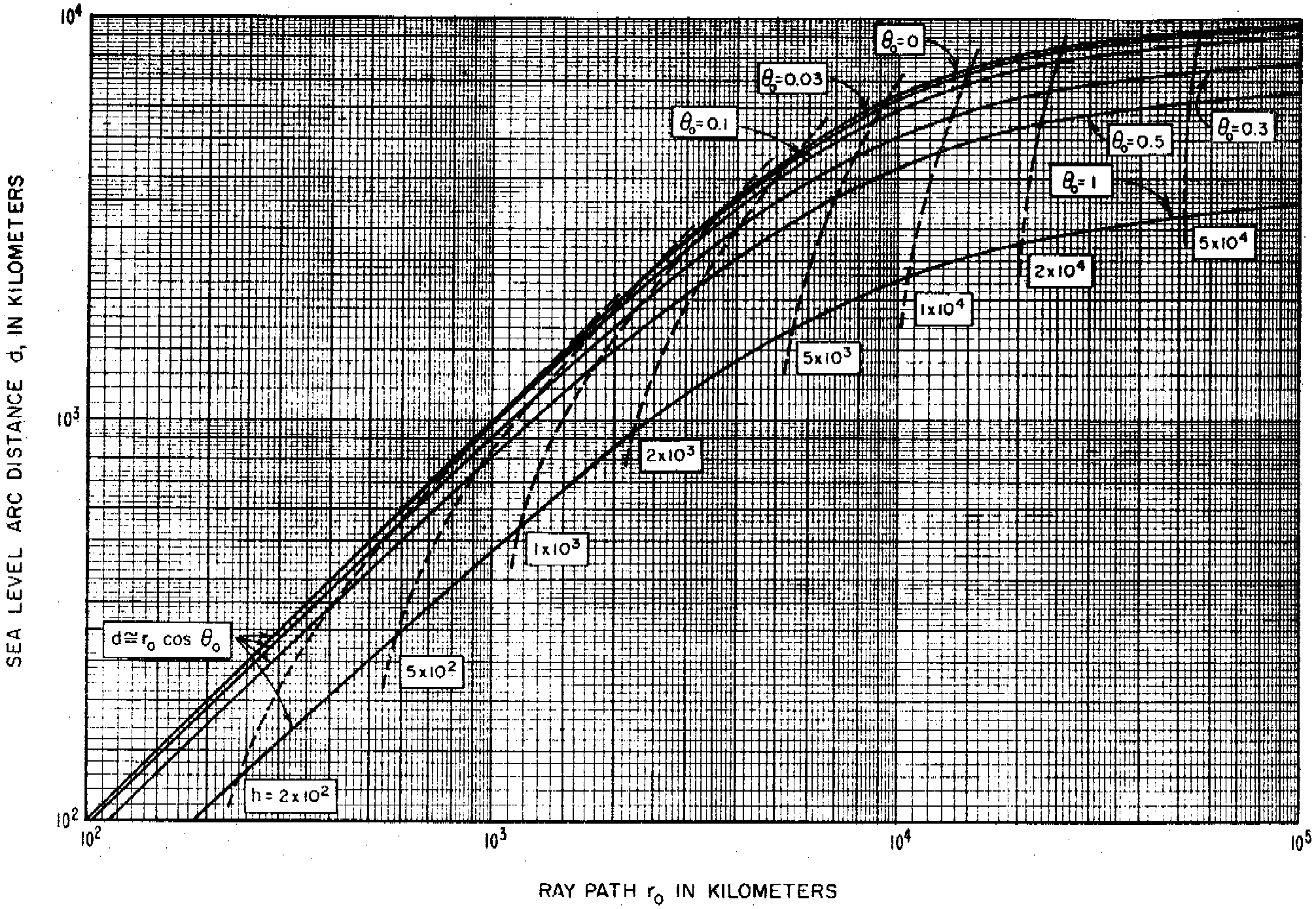

Figure 3.5

ESTIMATE OF MEDIAN OXYGEN AND WATER VAPOR ABSORPTION
FROM AUGUST DATA, WASHINGTON, D. C.

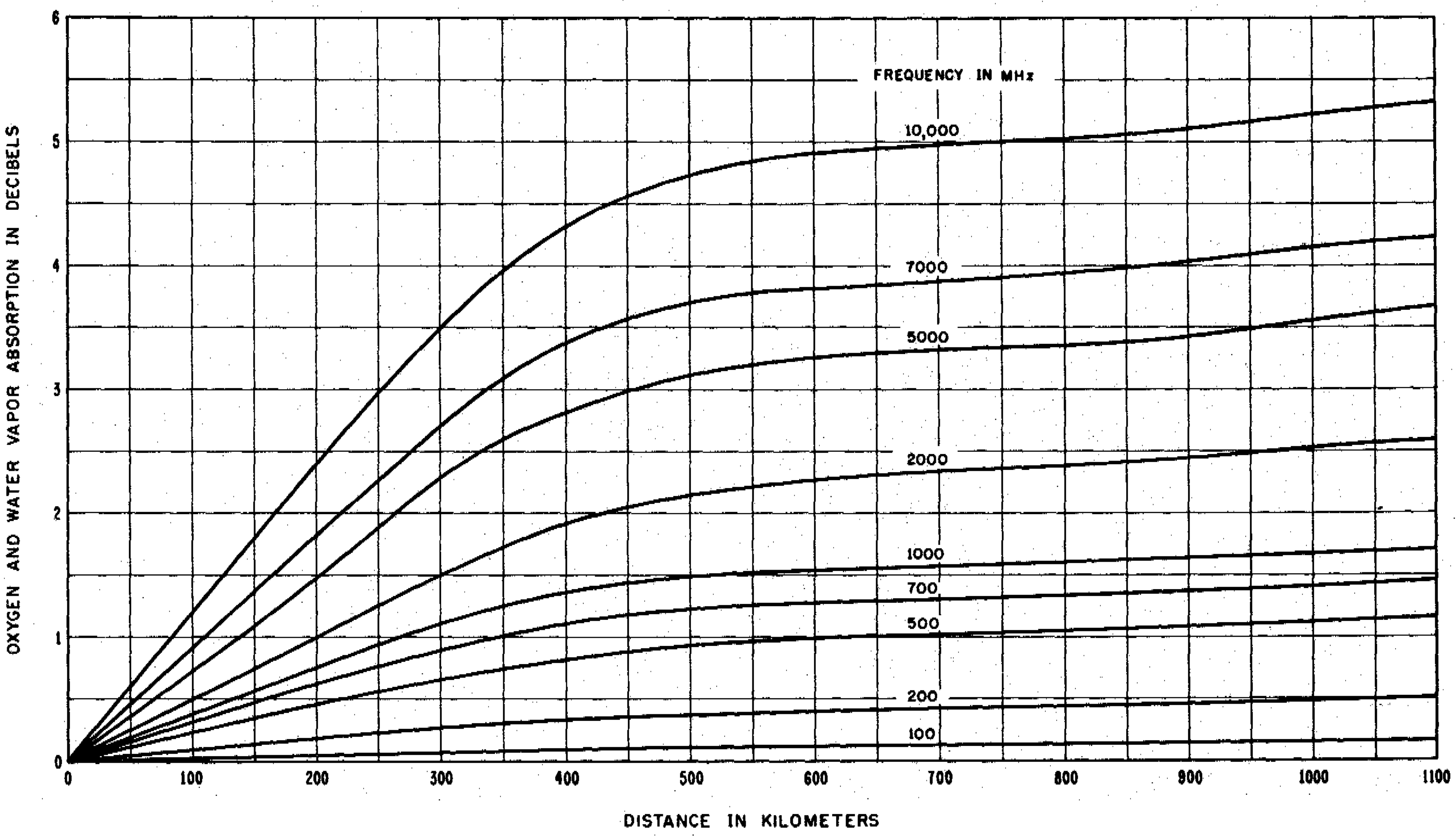

Figure 3.6

SKY NOISE TEMPERATURE DUE TO RERADIATION BY OXYGEN AND WATER VAPOR

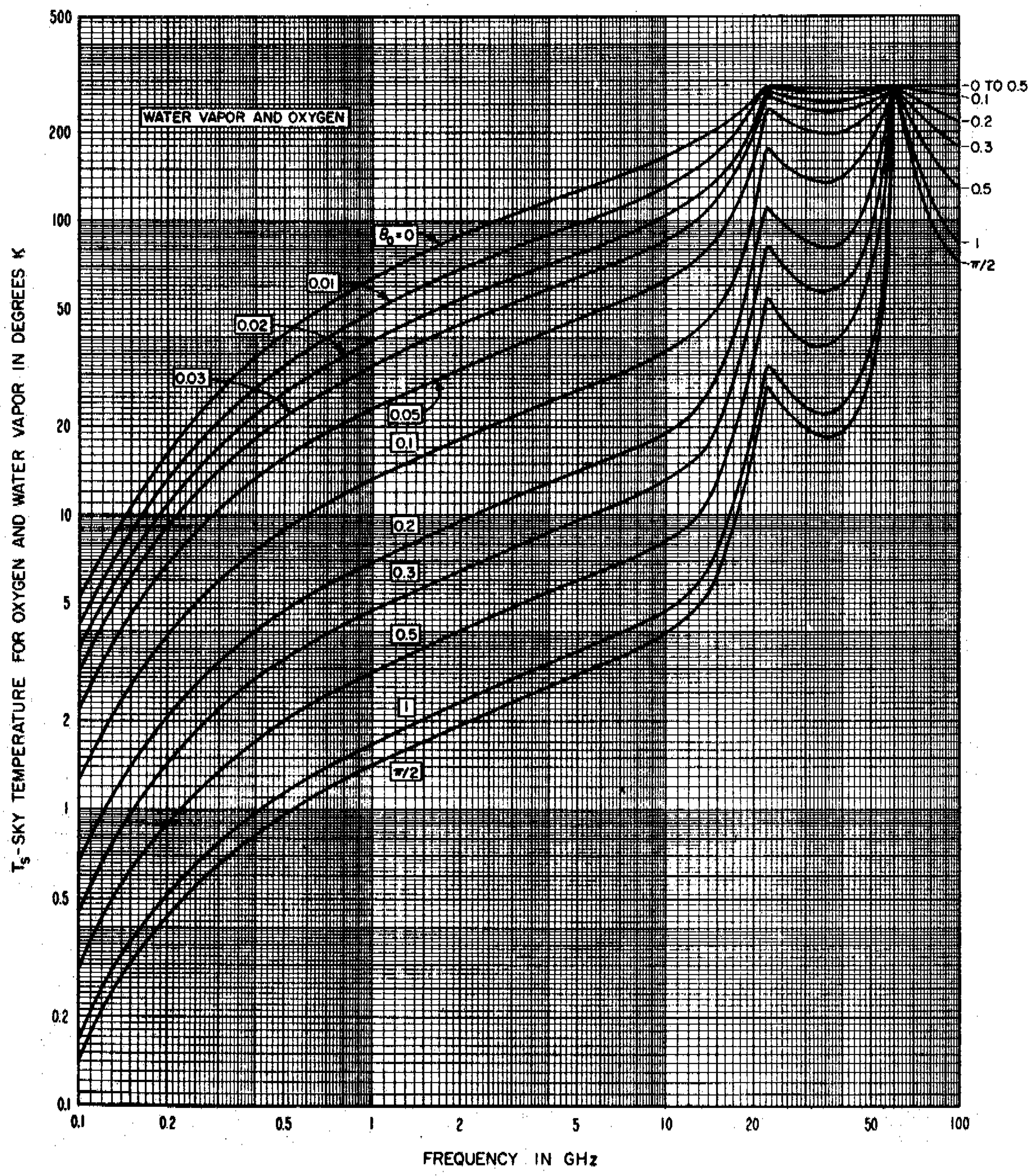

Figure 3.7

RAINFALL ABSORPTION COEFFICIENT K vs FREQUENCY

$\gamma = KR_r^{\alpha}$ db/km, WHERE R_r IS THE RAINFALL RATE IN MILLIMETERS/HOUR

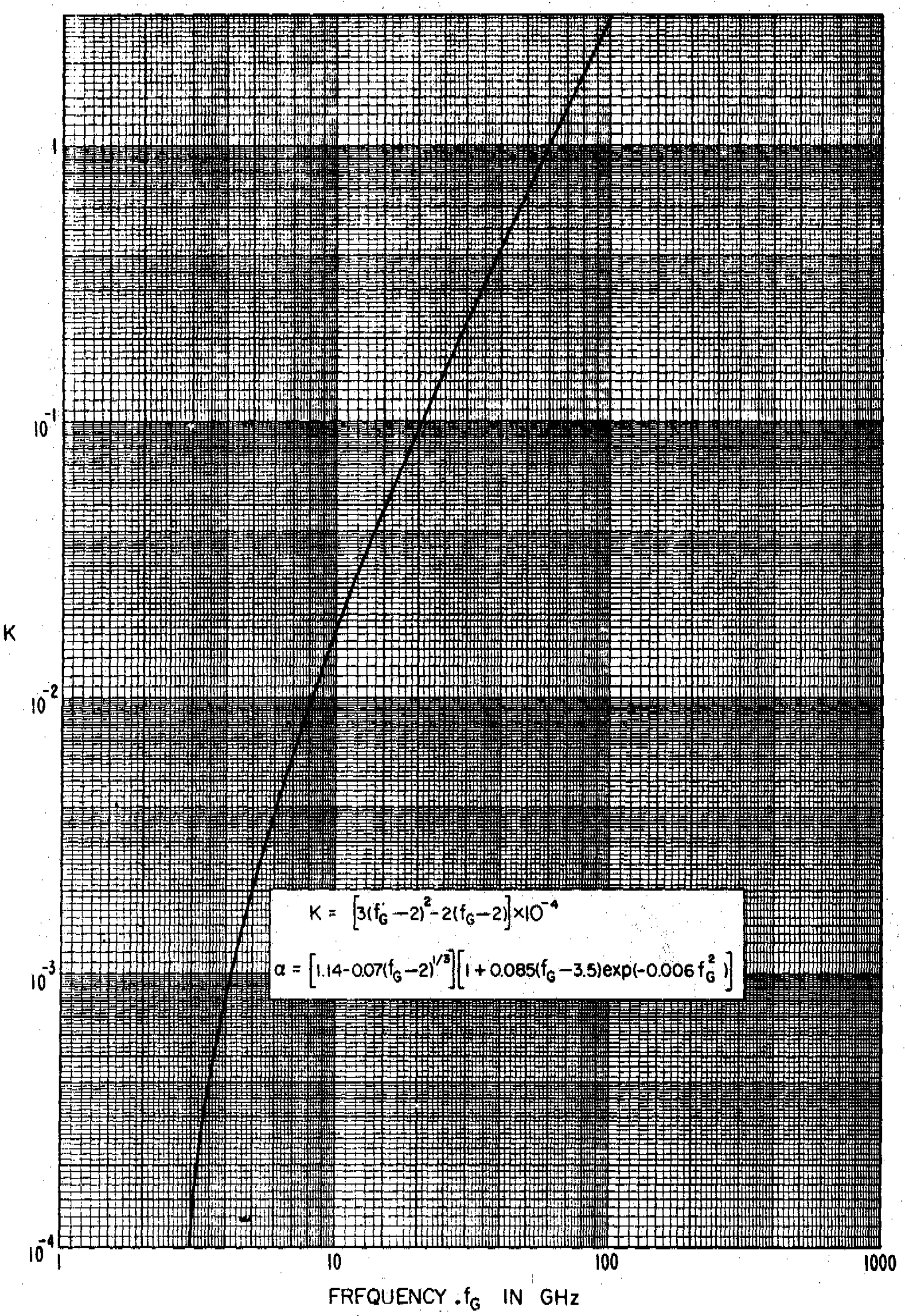

Figure 3.8

RAINFALL ABSORPTION EXPONENT α VS FREQUENCY

$\gamma = KR_r^{\alpha}$ db/km, WHERE R_r IS THE RAINFALL RATE IN MILLIMETERS/HOUR

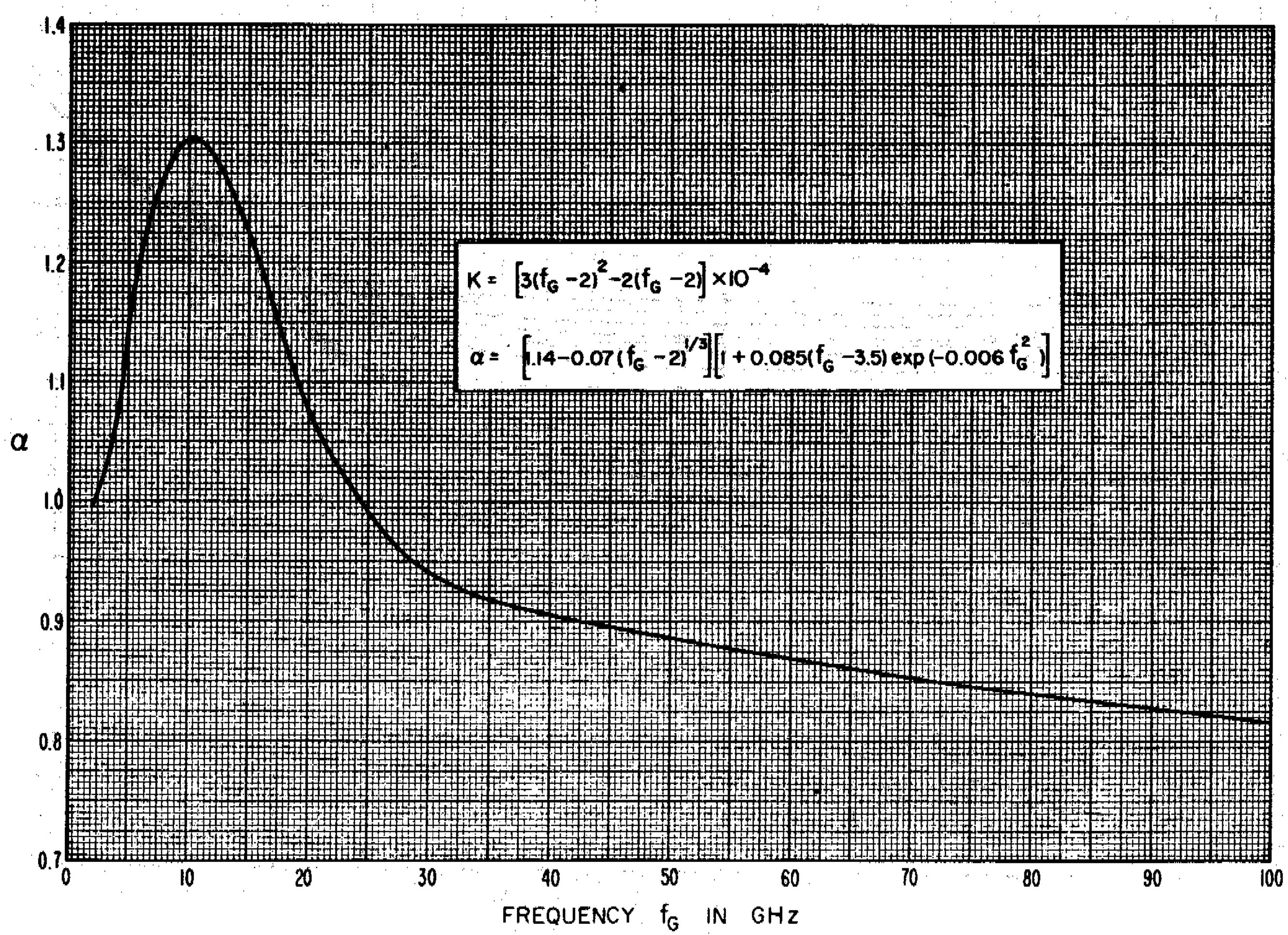

Figure 3.9

EFFECTIVE DISTANCE r_{er} FOR RAIN ABSORPTION

$\theta_0 = 0,\ 0.01,\ 0.02$

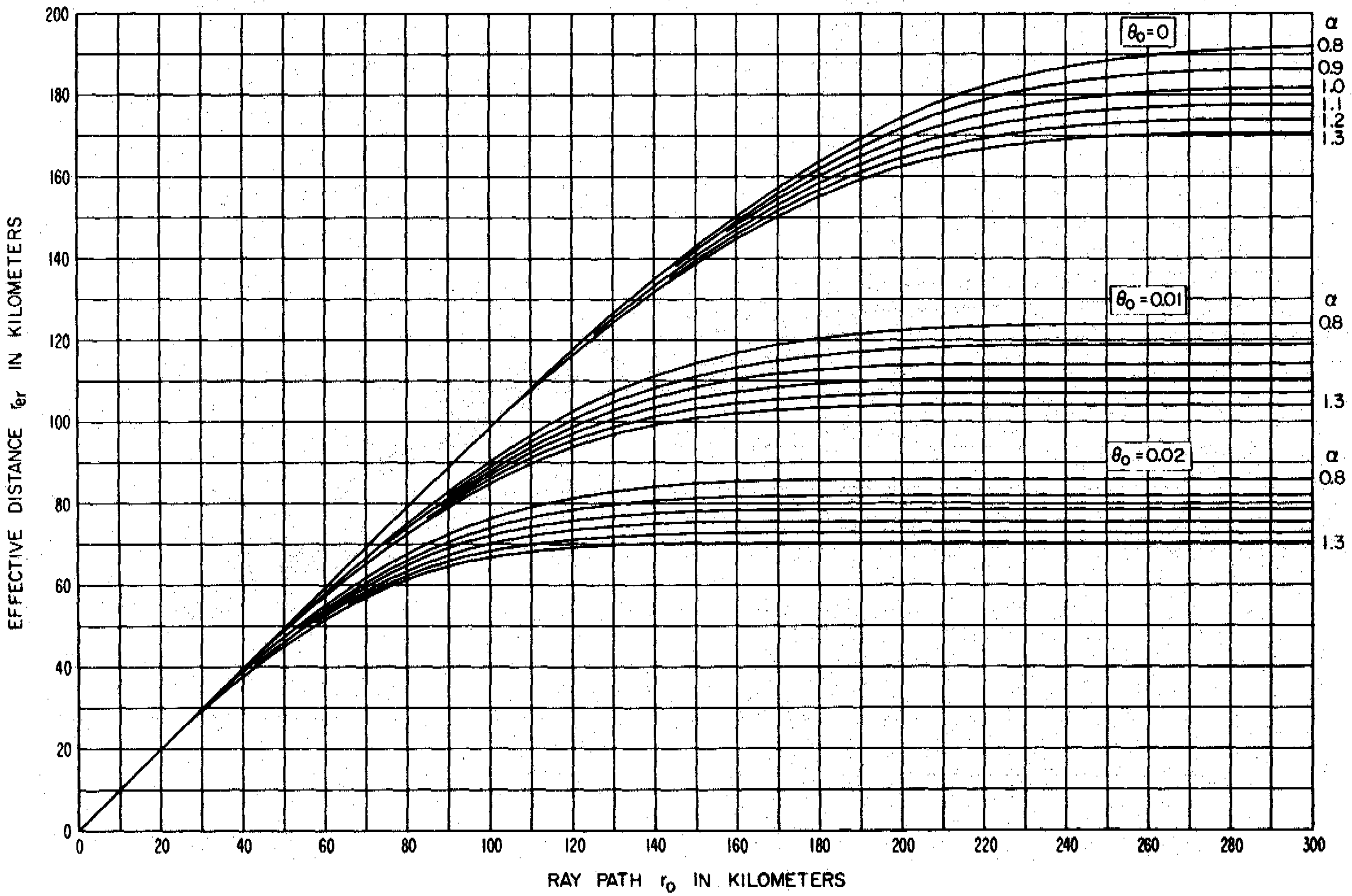

Figure 3.10

EFFECTIVE DISTANCE r_{er} FOR RAIN ABSORPTION

θ_0=0.05, 0.1, 0.2

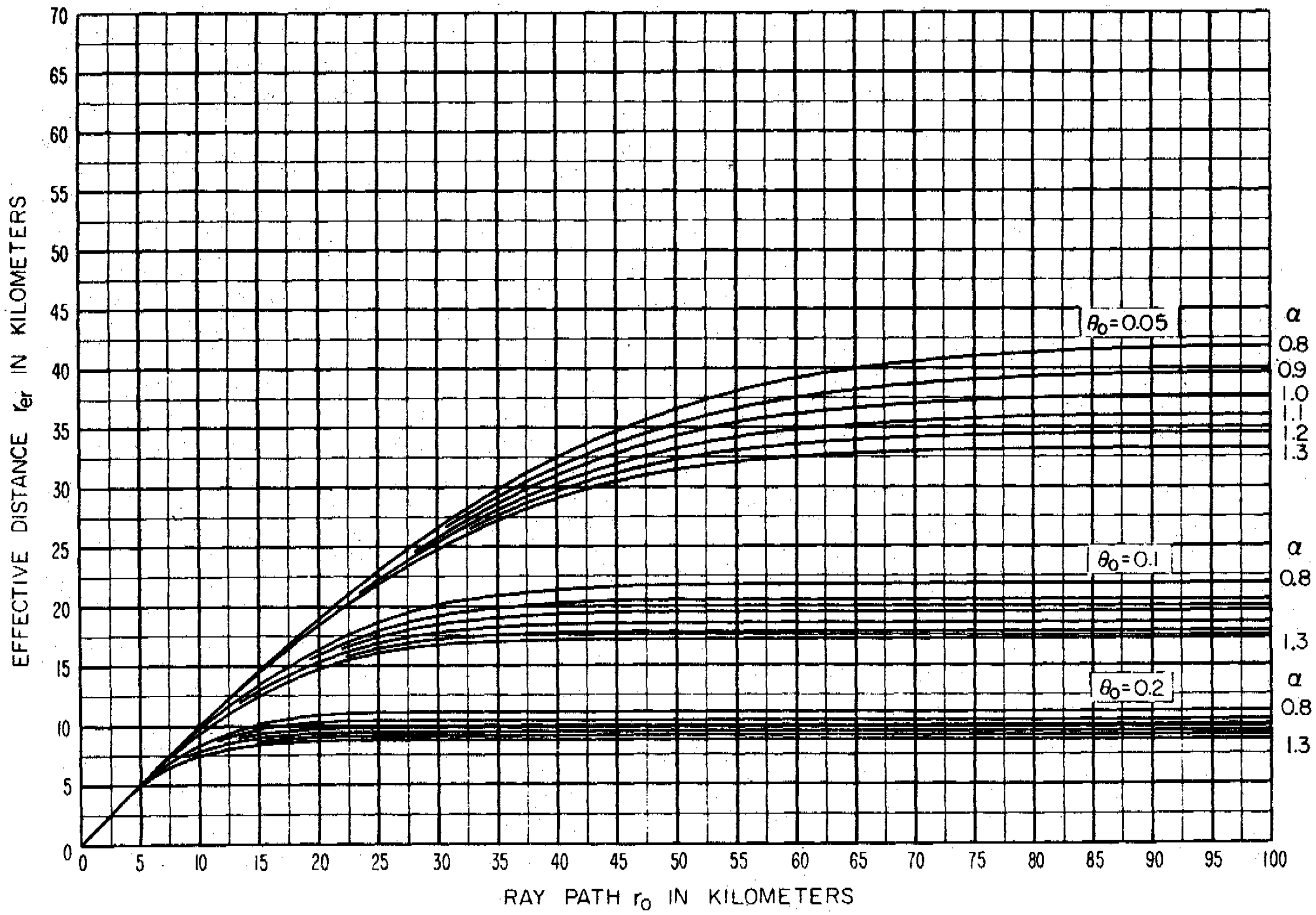

Figure 3.11

EFFECTIVE DISTANCE r_{er} FOR RAIN ABSORPTION

θ_0 = 0.5 AND 1

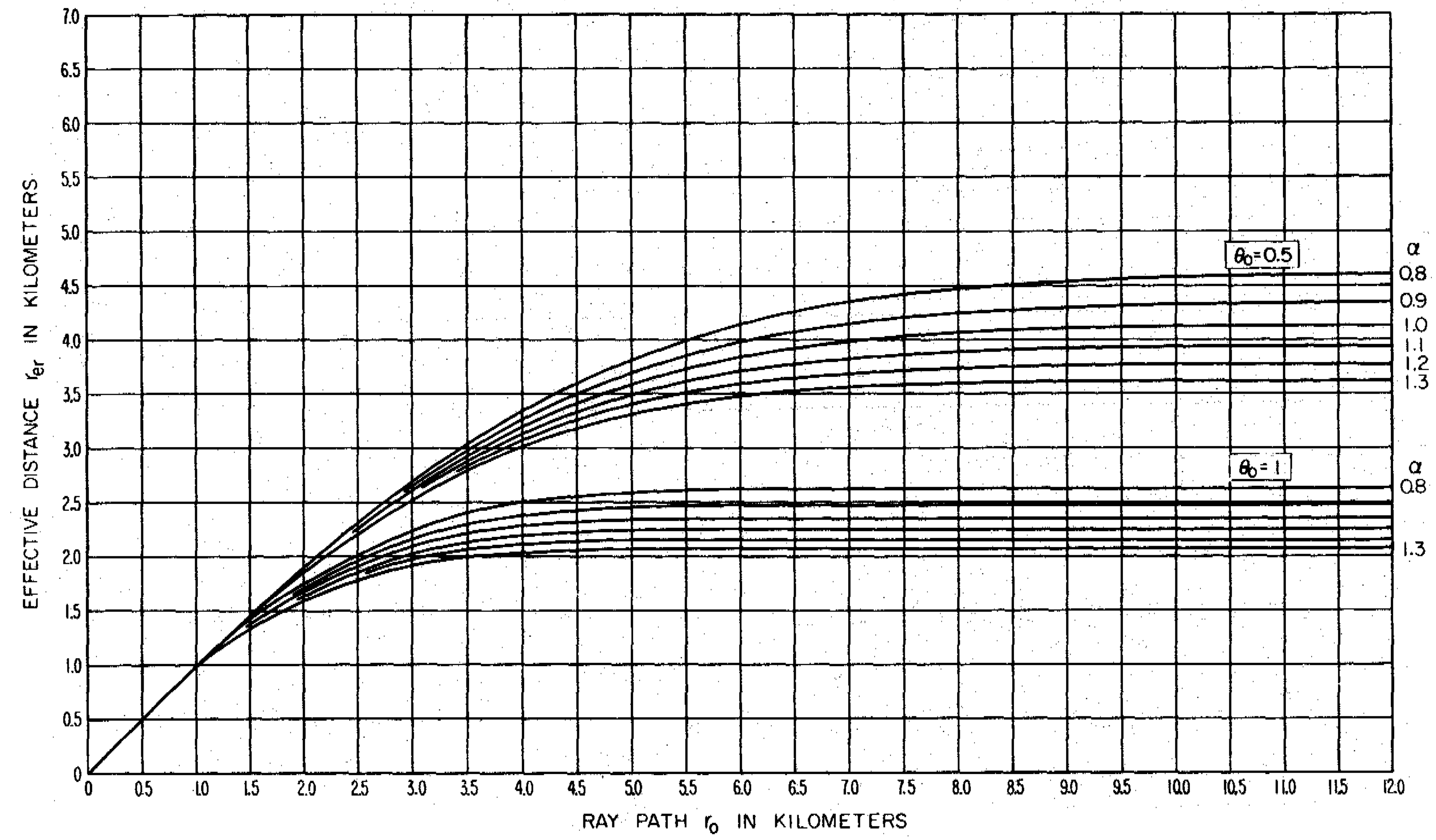

Figure 3.12

EFFECTIVE DISTANCE r_{er} FOR RAIN ABSORPTION

$\theta_0 = \pi/2$

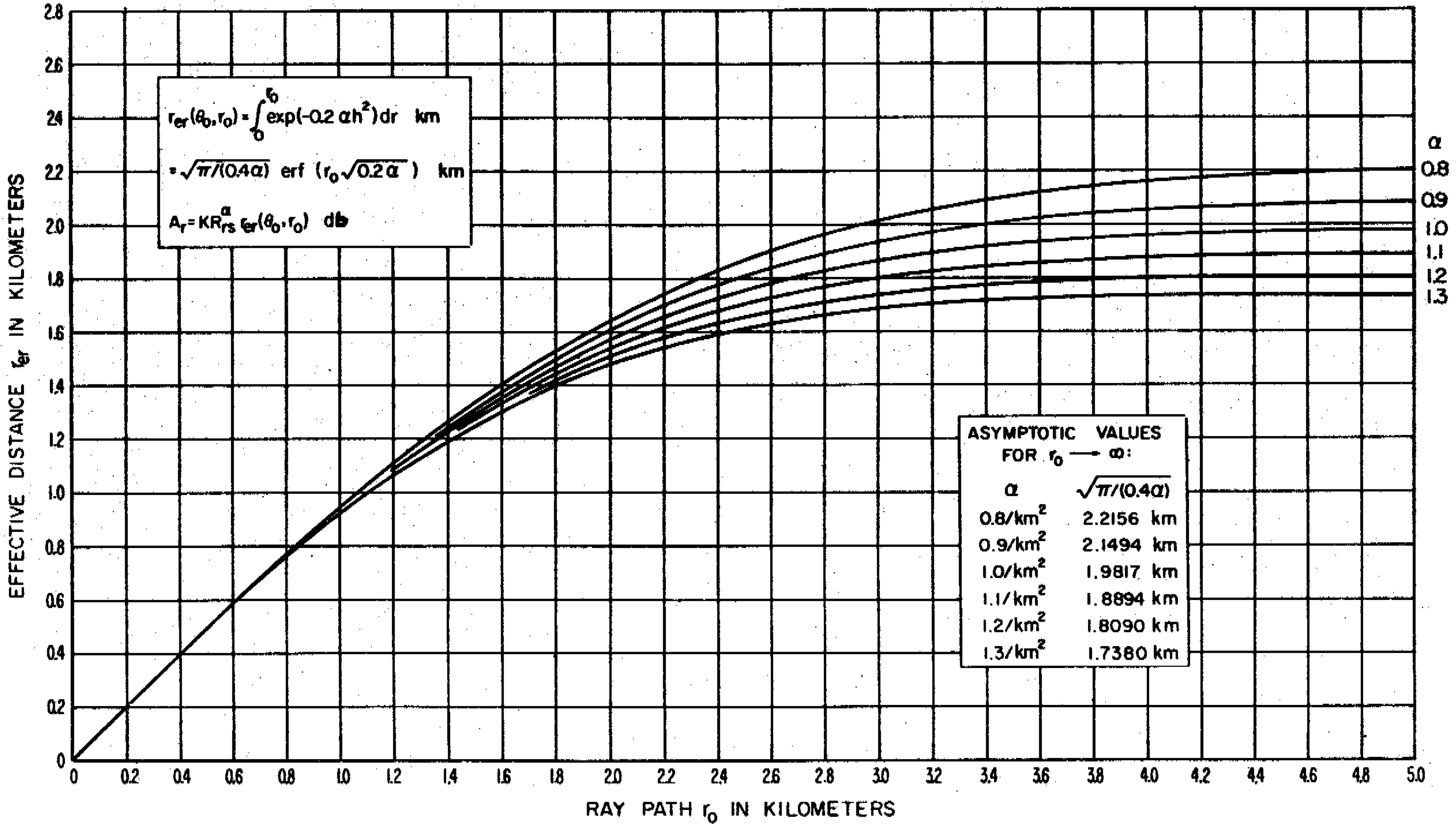

Figure 3.13

PATH AVERAGE RAINFALL RATE, $\overline{R}_r$, VS EFFECTIVE RAINBEARING DISTANCE, r_{er}
(TOTAL ANNUAL RAINFALL, 100 cm)

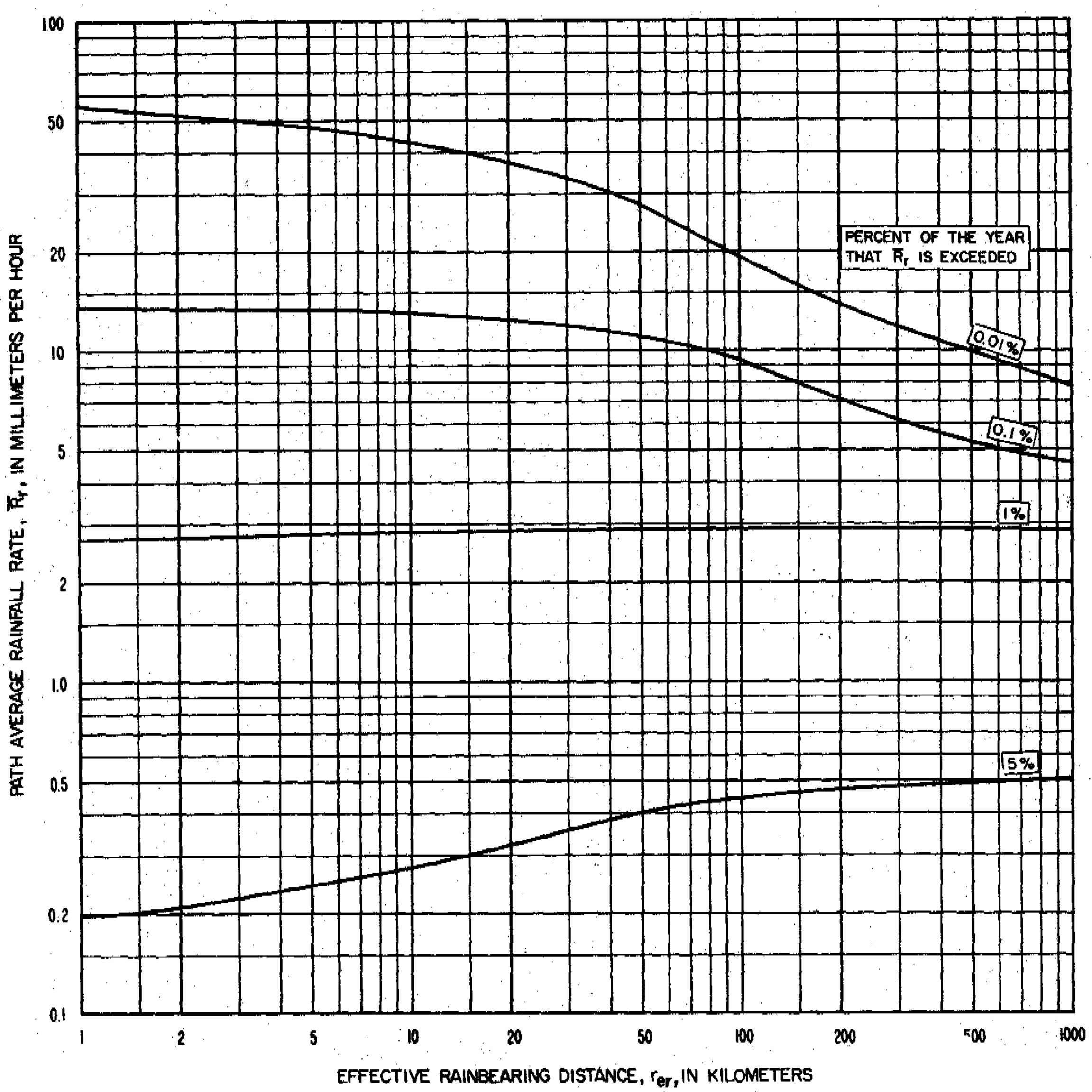

Figure 3.14